

Article

Effects of Superplasticizer and Water–Binder Ratio on Mechanical Properties of One-Part Alkali-Activated Geopolymer Concrete

Thanh-Tung Pham ¹, Ngoc-Linh Nguyen ¹, Tuan-Trung Nguyen ¹, Trung-Tu Nguyen ² and Thai-Hoan Pham ^{1,*}

¹ Faculty of Building and Industrial Construction, Hanoi University of Civil Engineering, Hanoi 12400, Vietnam; tungpt@huce.edu.vn (T.-T.P.); linhnn@huce.edu.vn (N.-L.N.); trungnt2@huce.edu.vn (T.-T.N.)

² Department of Civil and Environmental Engineering, Colorado State University, Fort Collins, CO 80523-1372, USA; nttu@crimson.ua.edu

* Correspondence: hoanpt@huce.edu.vn; Tel.: +84-904939887

Abstract: This study presents an investigation of the mix proportion and mechanical properties of one-part alkali-activated geopolymer concrete (GPC). The procedure for determining the mix proportion of one-part alkali-activated GPC, which uses a solid alkali activator in crystal form, is proposed. The proposed procedure was applied to a series of mixed proportions of GPC with different amounts of solid crystalline alkali activator (AA), water (W), and superplasticizer (SP), using the ratio between them to the total amount of binder (B, fly ash, and granulated blast furnace slag) by weight in order to evaluate their effect on the workability and compressive strength of the GPC. The slump, compressive and tensile strength, and elastic modulus of the one-part alkali-activated GPC were tested in various ways. The test results showed that solid crystalline alkali activators, water, and superplasticizers have significant effects on both the workability and compressive strength of GPC. The amount of one-part alkali activator should not exceed 12.0% of the total binder amount by weight (AA/B = 0.12) in order not to lose the workability of GPC. The minimum W–B ratio should be at least 0.43 to ensure the workability of the sample when no superplasticizer is added. An amount of 2.5% can be considered as the upper bound when using superplasticizer-based polysilicate for GPC. In addition, the elastic modulus and various types of tensile strength values of the one-part alkali-activated GPC were evaluated and compared with that predicted from compressive strength using equations given by two common ACI and Eurocode2 codes for ordinary Portland cement (OPC) concrete. Modifications of the equations showing the relationships between splitting tensile strength and compressive strength, as well as between elastic modulus and compressive strength and the development of compressive strength under the time provided by ACI and Eurocode2 for OPC concrete, were also made for one-part alkali-activated GPC.

Keywords: geopolymer concrete; crystalline alkali activator; fly ash; GBFS; workability; mechanical properties



Citation: Pham, T.-T.; Nguyen, N.-L.; Nguyen, T.-T.; Nguyen, T.-T.; Pham, T.-H. Effects of Superplasticizer and Water–Binder Ratio on Mechanical Properties of One-Part Alkali-Activated Geopolymer Concrete. *Buildings* **2023**, *13*, 1835. <https://doi.org/10.3390/buildings13071835>

Academic Editor: Jan Fořt

Received: 28 June 2023

Revised: 13 July 2023

Accepted: 16 July 2023

Published: 20 July 2023



Copyright: © 2023 by the authors. Licensee MDPI, Basel, Switzerland. This article is an open access article distributed under the terms and conditions of the Creative Commons Attribution (CC BY) license (<https://creativecommons.org/licenses/by/4.0/>).

1. Introduction

The large amount of carbon dioxide (CO₂) emitted from industrial activities every year is one of the causes of global warming. The cement industry accounts for 5–7% of the total CO₂ emitted, and this number will continue to increase rapidly in the near future due to the increasing demand for ordinary Portland cement (OPC) [1]. Therefore, the research towards the development and manufacture of new environmentally friendly alternatives to OPC is essential and has interested scientists in recent times. Geopolymer (GP) is one of the new types of binder with many advantages and has the potential to replace ordinary Portland cement, especially in concrete fabrication, with a new concrete called geopolymer concrete (GPC) [2]. GPC was studied as early as 1908; important studies of Glukhovskiy [3], Krivenko [4], and Davidovits [5] followed in which the concept of “geopolymer binder” was

officially introduced by Davidovits [5], providing the basic theory of this type of concrete. The basic theory of GPC has been the subject of numerous studies carried out to investigate its crystal structure as well as its mechanical and microstructural properties [6,7]. For instance, Kim et al. [7] pointed out that GPC completely meets the technical requirements of the main mechanical properties, similar to OPC. Moreover, GPC has more outstanding features, such as high fire resistance and corrosion resistance in aggressive environments [8–10] and thermal conductivity [11–13]. Concerning the application of GPC to building, this material was used in Mariupol, Ukraine, in the 1960s to build two nine-story residential buildings, while the first residential building made of alkali-activated concrete without any Portland cement was built in 1989 in Liepensk, in the Russian Federation, and has 20 floors [14].

As indicated by Davidovits [15], the two main components needed for making GPC are rich aluminate (Al) and silicate (Si) materials and an alkali-activator (AA) source to create an alkaline environment. Sources of rich Al and Si materials for GPC production are usually by-products from steel mills and thermal power plants, such as fly ash (FA), granulated blast furnace slag (GBFS), silica fume (SF), and red mud. There have been a number of studies on the influence of these raw materials on the behavior and performance of GPC [16–24]. For example, Davidovits [21] and Hajjaji et al. [16] manufactured GPC that had a compressive strength of up to 80 MPa when heat cured by using only FA as the source material for GPC. Other investigations pointed out that replacing a part of FA by GBFS and SF in GPC leads to several advantages, such as decreased setting time, increased workability, compressive strength of GPC, and notably, that GPC can be cured at room temperature to achieve high intensity when using GBFS. On the other hand, the alkali activators commonly used to create an alkaline environment during the polymerization reaction are NaOH and KOH; however, these strong alkalis are often combined with liquid glass solutions to avoid danger and to achieve easy GPC manufacture [25].

Currently, there are two commonly used types of activators: liquid and solid crystalline. A liquid activator is made by dissolving pure NaOH crystals into water to form a NaOH (alkaline) solution and then mixing it with sodium hydroxide (SH) liquid glass. This type of activator has been widely used due to the ease of making AA solutions from available popular materials. The effects of liquid activator characteristics, such as the molar concentration of NaOH solution and the ratio NaOH/Na₂SiO₃, on the workability, compressive strength, and some other mechanical properties of GPC have been investigated [26,27]. However, liquid activator has some disadvantages, such as being suitable only for precast concrete structures, because the AA solution needs to be prepared long before proceeding to manufacture GPC, and there is a high level of danger in direct contact with strong alkaline solutions during GPC fabrication.

Recently, solid crystalline AA has been more widely used because of its many advantages in making GPC, such as convenience in the manufacturing process (similar to cement), easy transportation, and suitability for on-site construction. The current common fabrication of solid crystalline AA (so-called one-part alkali activator) involves heating the solid silicate (SiO₃²⁻) raw material and the alkali (Na⁺) source at a high temperature before the one-part alkali-activated geopolymer paste is mixed by adding aggregates, additional alumina and/or silica sources, additives, and fiber following the procedure shown in Figure 1 [28]. In this procedure, the ratio of SiO₂/Na₂O is normally fixed depending on the manufacturer. As indicated by Hajimohammadi et al. [29] and Nematollahi et al. [30], this ratio can be ranged from 0.93 to 3.32. Similar to liquid AA, using solid crystalline AA for GPC is also affected by many factors, such as the Al₂O₃/SiO₂ ratio of the source material, FA/GBFS, AA/B (binder), and H₂O/B ratios. However, due to the fixed SiO₂/Na₂O ratio of the solid AA, the amount of water (H₂O/Na₂O) thus greatly affects the alkali concentration, influencing GPC's compressive strength. In addition, the type and amount of superplasticizer (SP) is one of the important factors in reducing the amount of water used and ensuring workability during GPC fabrication [30].

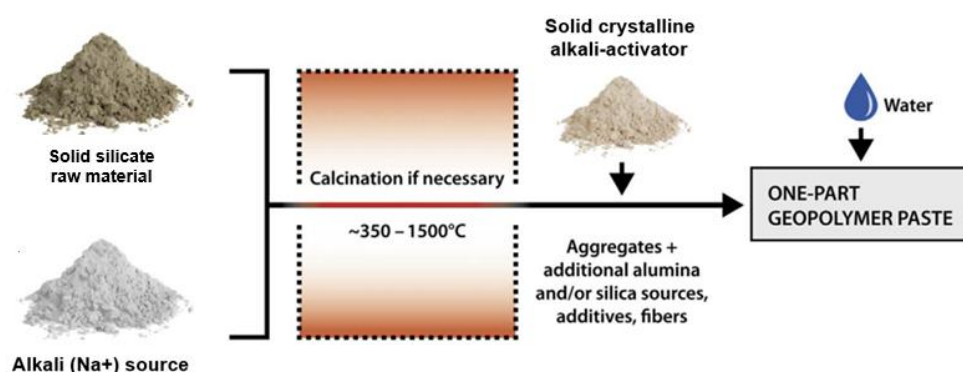


Figure 1. Fabrication of one-part alkali-activated geopolymer paste from solid AA.

In this study, the mixed proportion procedure of GPC using solid crystalline AA (so-called one-part alkali-activated GPC) is proposed. The workability and mechanical properties of one-part alkali-activated GPC with different AA/B, H_2O/Na_2O , W/B, and SP ratios are investigated. The relationship between compressive strength and different types of tensile strength, as well as between compressive strength and elastic modulus of GPC, is also evaluated.

2. Experimental Program

2.1. Materials

The fly ash (FA) used in this study is F-class, which was collected, dried, and packed from a local thermal power plant in Vietnam (Figure 2a). The granulated blast furnace slag (GBFS) was finely ground, dried, and packed from a local steel factory in Vietnam (Figure 2b). Both materials were tested for chemical composition and particle size before being used. The analysis results of the fly ash and blast furnace slag samples showed that these materials satisfy the requirements of EN 196-1 [31]. Table 1 lists the physical properties and chemical composition, while Figure 3 presents the XRD analysis results of the FA and GBFS.

Table 1. Properties of fly ash and granulated blast furnace slag.

	FA	GBFS
Physical properties		
Density (kg/m^3)	2240	2910
Surface area (cm^2/g)	3400 (Blaine)	5220 (Blaine)
Chemical composition (%)		
SiO_2	58.70	35.02
Al_2O_3	22.87	13.56
Fe_2O_3	7.31	1.41
CaO	0.98	38.6
MgO	0.85	8.18
Na_2O	0.33	0.31
K_2O	3.6	0.80
TiO_2	1.35	0.23
MKN	3.53	1.89

Crystalline hydrated sodium silicate salt with a density of $2410 kg/m^3$ and the SiO_2/Na_2O composition ratio by mass of 2.1 was used as a one-part alkali-activator. The image and XRD analysis result of solid crystalline one-part alkali-activator are shown in Figure 4. Crushed stone with a grain size of 5–10 mm and river sand were used as the coarse and fine aggregate materials. The physical properties of stone and sand are presented in Table 2.



Figure 2. Fly ash and granulated blast furnace slag: (a) fly ash; (b) granulated blast furnace slag.

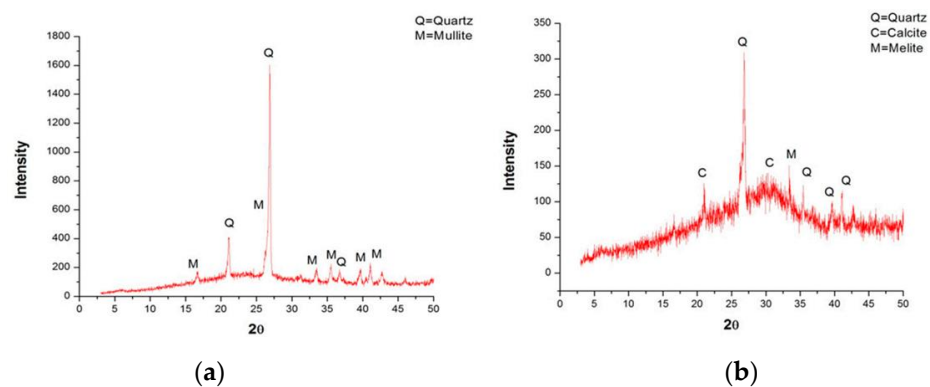


Figure 3. XRD analysis results of fly ash and granulated blast furnace slag: (a) fly ash; (b) granulated blast furnace slag.

Table 2. Properties of stone and sand.

	Stone	Sand
Density in dry condition (kg/m^3)	2730	2630
Density at surface dry saturation (kg/m^3)	2760	2650
Volumetric mass in the compacted state (kg/m^3)	1586	1700
Porosity in compacted state (%)	42.9	35.0
Surface dry saturated water absorption (%)	0.84	0.75

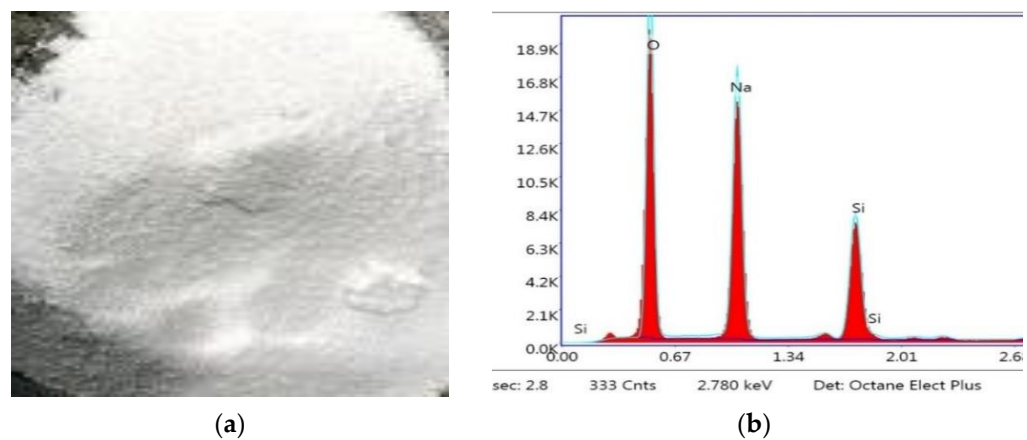


Figure 4. (a) Solid crystalline alkali-activator; (b) XRD analysis result of alkali-activator.

For GPC in this study, a ROADCON-SSA3000 based on active polyethylene glycol methacrylate was used as a superplasticizer (SP) to ensure compliance with ASTM C494/C494M D and G standards [32].

2.2. Mix Proportion

There are some principles for the determination of mixed proportion of GPC; however, they mainly focus on GPC using liquid activators. The composition ratios for GPC using fly ash source materials and liquid activators were given by Davidovits [5] such as the liquid activators/binder ratio from 0.3 to 0.45, sodium silicate/sodium hydroxide ratio from 2.0 to 2.5, and the water–binder ratio from 0.16 to 0.24 with an important assumption that the density of GPC is 2400 kg/m^3 . The mix proportion then needs to be adjusted as the density is highly dependent on the type of aggregate used. The instructions for calculating the mix proportion of GPC using a solid crystalline alkali-activator are quite few. For simplicity and ease of application, the calculation of the mixed proportion of GPC in this study is based on the paste thickness of coated aggregate and the close bulk packing theory [33], together with some adjustments to make it suitable for solid crystalline one-part alkali-activator. The procedure for determining the mix proportion of GPC using a solid crystalline one-part alkali-activator consists of the following steps:

Step 1. Determining the optimal aggregate ratio.

The optimal fill between the used aggregates is determined based on the particle distribution curve of each aggregate type. According to the method given in ASTM C29 [34], the ratio between sand and (sand + stone) can be specified to be 0.39 from the particle distribution curve of sand and stone using Equation (1) as:

$$X = \alpha_1 x_1 + \alpha_2 x_2 + \alpha_3 x_3 + \alpha_4 x_1 x_2 + \alpha_5 x_2 x_3 + \alpha_6 x_1 x_3 + \alpha_7 x_1 x_2 \quad (1)$$

where X is the bulking density of combined (sand + stone) aggregate (in kg/m^3), α_i is the interaction coefficient of aggregate, and x_i is the mass fraction of aggregates with different size (in %).

Step 2. Determining the paste thickness of coated aggregate.

The paste thickness of coated aggregate or the amount of mortar used is determined based on the principle of absolute total volume or by calculating the amount of mortar from the total area of aggregate using Equation (2) as:

$$V_p = t \cdot (\beta_s M_s A_s + \beta_g M_g A_g) + V_b \quad (2)$$

where V_p is the total volume of mortar required (the unit volume of the geopolymer paste); t is the paste thickness that was homogeneously coated on the surface of an aggregate (in μm); β_s and β_g are the correction coefficients, which were introduced to reduce the sharp errors of aggregate between the ideal sphere and the real sharp and were taken as 1.05 and 1.12 for river sand and coarse aggregate, respectively [33]; M_s and M_g are the mass of the fine and coarse aggregates (in kg), respectively; A_s and A_g are the specific surface area of fine and coarse aggregates (in m^2/kg), respectively; and V_b is the mortar volume between aggregate particles, which is calculated as follows:

$$V_b = \frac{M_s}{\rho_s} \left(1 - \frac{\rho_s'}{\rho_s}\right) \quad (3)$$

In Equation (3), ρ_s and ρ_s' are the packing density and apparent density of aggregates, respectively (in kg/m^3). From the volume of paste thickness of coated aggregate, the amount used of source materials, including FA and GBFS, can be calculated. In this study, the total amount used of FA and GBFS was determined to be $400 \text{ kg}/(\text{m}^3 \text{GPC})$.

Step 3. Determining aluminum and silicate source ratio.

Currently, there are many sources of Aluminum and Silicate that are used for GPC, such as fly ash, granulated blast furnace slag, metakaolin, and red mud. However, it has been suggested that FA and GBFS should be used for one-part alkali-activated GPC [25]. Using granulated blast furnace slag plays an important role in early age formation and does not require heat curing for GPC. At the same time, the use of fly ash plays an important role in long-term age formation and in saline environments [16]. The ratio of $\text{SiO}_2/\text{Al}_2\text{O}_3$

from the source materials for liquid activators is about 3.3 to 4.5, while for dry activators is about 0.75 to 6.02 [21]. The selection of the ratio between FA and GBFS has been carried out to evaluate the influence on workability and properties of GPC [17,18]. In this study, the ratio of FA-GBFS of 1:3 was chosen with the expectation that the GPC does not need heat curing and the strength at an early age of GPC can be improved.

Step 4. Determining the amount of one-part alkali-activator.

Determining the amount of liquid activator is said to be quite complicated due to the need to determine the type of sodium hydroxide with different molar concentrations and different amounts of water. However, for solid crystalline one-part alkali-activator, the ratio of $\text{Na}_2\text{O}/\text{SiO}_2$ is usually fixed by suppliers, together with the crystalline form, leading to no need to recalculate the amount of water in the solution when fabricating GPC with different grades. Therefore, when calculating the amount of solid crystalline one-part alkali-activator, it just needs to choose the required amount of Na_2O to be used to create an alkaline environment to break Al-O and Si-O connections in the source materials (the total amount of FA and GBFS).

In this study, the solid alkali-activator (AA) with the fixed $\text{SiO}_2/\text{Na}_2\text{O}$ ratio of 2.1 was used, and the ratio of solid AA to the source materials (FA + GBFS) was chosen to be 4%, 6%, 8%, 10%, and 12% by weight for the investigation.

Step 5. Determining the amount of water.

Unlike liquid activators, when the amount used of water greatly affects the workability and compressive strength of GPC, the amount used of water influences the pH level in GPC using the solid crystalline one-part alkali-activator with a fixed $\text{SiO}_2/\text{Na}_2\text{O}$ ratio of 2.1. Therefore, the $\text{H}_2\text{O}/\text{Na}_2\text{O}$ ratio is one of the important ratios when using a crystalline activator. In this study, the water-binder (W/B) ratio from 0.43 to 0.52 and the $\text{H}_2\text{O}/\text{Na}_2\text{O}$ ratio from 12.6 to 27.9 were investigated to evaluate the effect of these ratios on the workability and compressive strength of GPC.

Step 6. Determining the amount of superplasticizer.

Additives to reduce water or superplasticizers are normally used to increase workability as well as to reduce the amount of water used to improve the compressive strength of concrete. For conventional OPC concrete, additives based on lignosulfonates, naphthalene, melamine-based, and polycarboxylates are commonly used. However, some superplasticizers may lead to rapid hardening of GPC. As indicated [20,25,26], superplasticizers based on naphthalene and polycarboxylate sources can be used for GPC. In this study, the superplasticizer based on polyethylene glycol methacrylate was used. The content of superplasticizer by weight of 1%, 1.5%, and 2% (SP/B) was used to evaluate the effect of this additive on the workability and compressive strength of GPC.

The procedure for calculating the mix proportion of one-part alkali-activated GPC is summarized as shown in Figure 5. Following the proposed procedure, a series of mixed proportions of one-part alkali-activated GPC paste for the investigation is denoted with specific codes and provided in Table 3. The labels "AA", "W", and "SP" represent the solid alkali-activator, water, and superplasticizer, respectively. The first number, "0.04", "0.06", "0.08", "0.1", and "0.12", refers to the ratio of solid AA to the total binder (FA + GBFS) by weight (AA/B). The second number, "0.37", "0.39", "0.41", "0.43", "0.45", "0.48", and "0.52", refers to the ratio of water to the total binder (FA + GBFS) by weight (W/B). The third number (1.0–2.5) is the percentage of the superplasticizer to the total binder (FA + GBFS) weight (SP/B). It is noted that the $\text{H}_2\text{O}/\text{Na}_2\text{O}$ ratio was also changed according to the change of (AA/B) or (W/B). The series of mixed proportions was also divided into two groups, A and B. The mix proportions in group A were designed to investigate the effect of the AA/B ratio, whereas the ones in group B were designed to evaluate the effect of the W/B ratio on the workability and mechanical properties of GPC. For these purposes, the W/B ratio in group A was fixed at 0.45, while the AA/B ratio in group B was kept unchanged at 0.08.

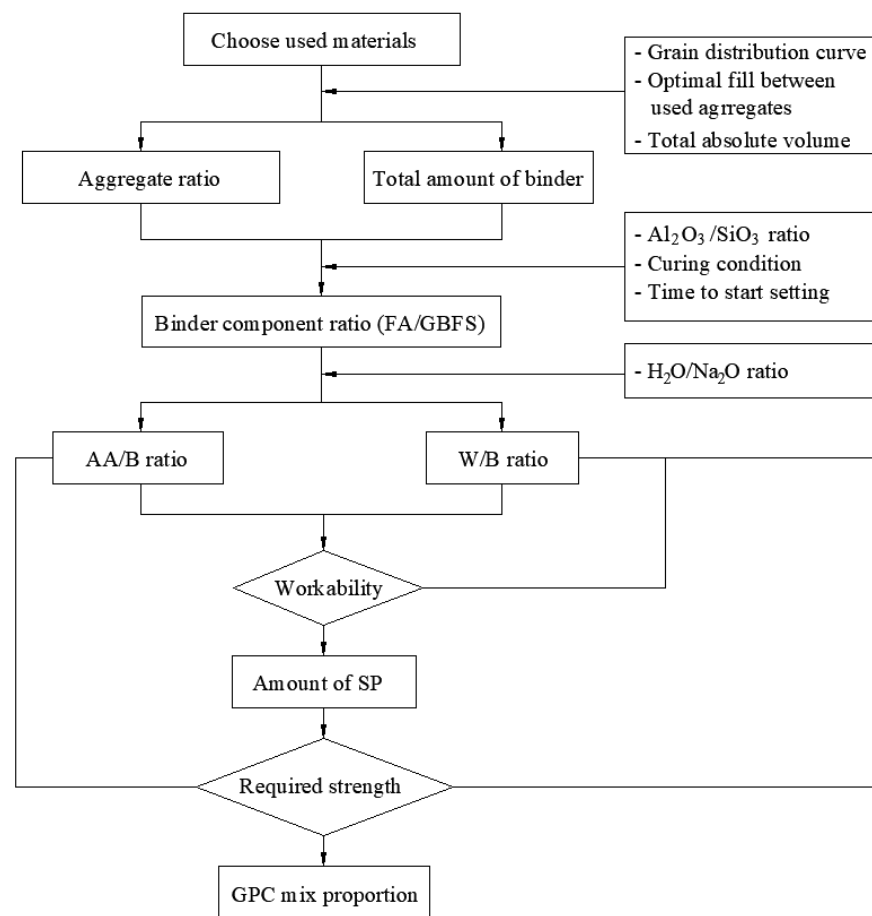


Figure 5. Procedure for calculating the mix proportion of one-part alkali-activated GPC.

Table 3. Mix proportions of one-part alkali-activated GPC.

Group	Specimens	FA (kg)	GBFS (kg)	Sand (kg)	Stone (kg)	AA (kg)	W (l)	Ratio			
								AA/B	W/B	H ₂ O/Na ₂ O	SP
A	AA0.04-W0.45	100	300	640	1220	16	180	0.04	0.45	27.90	0
	AA0.06-W0.45	100	300	640	1220	24	180	0.06	0.45	19.90	0
	AA0.08-W0.45	100	300	640	1220	32	180	0.08	0.45	17.44	0
	AA0.10-W0.45	100	300	640	1220	40	180	0.10	0.45	12.60	0
	AA0.12-W0.45	100	300	640	1220	48	180	0.12	0.45	10.80	0
B	AA0.08-W0.52	100	300	640	1220	32	208	0.08	0.52	23.09	0
	AA0.08-W0.48	100	300	640	1220	32	192	0.08	0.48	21.31	0
	AA0.08-W0.45	100	300	640	1220	32	180	0.08	0.45	17.44	0
	AA0.08-W0.43	100	300	640	1220	32	172	0.08	0.43	16.66	0
	AA0.08-W0.43-SP1.0	100	300	640	1220	32	172	0.08	0.43	16.66	1.0
	AA0.08-W0.41-SP1.0	100	300	640	1220	32	164	0.08	0.41	15.12	1.0
	AA0.08-W0.41-SP1.5	100	300	640	1220	32	164	0.08	0.41	15.12	1.5
	AA0.08-W0.39-SP1.5	100	300	640	1220	32	156	0.08	0.39	13.96	1.5
	AA0.08-W0.39-SP2.0	100	300	640	1220	32	156	0.08	0.39	13.96	2.0
	AA0.08-W0.37-SP2.0	100	300	640	1220	32	148	0.08	0.37	12.15	2.0
AA0.08-W0.37-SP2.5	100	300	640	1220	32	148	0.08	0.37	12.15	2.5	

2.3. Experimental Details

One-part alkali-activated GPC was produced at room temperature as follows: First, the aggregate composition was quantified. The dry fly ash, blast furnace slag, sand, and solid alkali-activator were mixed for 2 min and then activated by adding 70% water. An

additional two-minute mixing time was carried out to homogenize the mixture. Finally, the stone (coarse aggregate) and the remaining 30% water were added and subsequently proceeded to mix for another two minutes.

The workability of the GPC was evaluated by conducting slump tests for fresh one-part alkali-activated GPC according to the ASTM C143-78 [35]. The prepared fresh one-part alkali-activated GPC of each mixture was cast into three 100 mm × 200 mm cylindrical molds, and then the slump test was carried out, as illustrated in Figure 6.



Figure 6. Slump test of GPC.

For other tests, the fresh pastes of each mixture were cast into the corresponding molds, and all GPC molds were covered with plastic sheets and cured in a laboratory. The humidity and temperature in the laboratory were kept stable for 24 h until the molds were removed for all specimens. The specimens were then continued to be covered with plastic sheets in the same conditions to avoid dehydration and stabilize the temperature inside the specimens until the testing days.

Compressive strength tests were conducted using a universal testing machine according to ASTM C39 [36] at 3, 7, and 28 days for all GPC mix proportions. After the compressive strength tests, three mix proportions that showed the compressive strength of about 30 MPa, 40 MPa, and 50 MPa were chosen to investigate the tensile strength and modulus of elasticity as well as their relations with the compressive strength. The static modulus of elasticity was calculated based on the stress corresponding to 40% of the ultimate load according to ASTM C469-10 [37]. The tensile strength of GPC was investigated through three testing types, including flexural tensile strength, splitting tensile strength, and axial (direct) tensile strength tests, according to ASTM C78-18 and ASTM C496-04 [38,39]. The list of testing types, the shape and size of the specimen for each testing type, and the testing day are presented in Table 4.

Table 4. Testing and specimen details.

Testing Type	Specimen Shape and Size (mm)	Day of Testing	Illustration
Compressive strength	Cylinder 150 × 300	3, 7, 28	

Table 4. Cont.

Testing Type	Specimen Shape and Size (mm)	Day of Testing	Illustration
Flexural tensile strength	Prism 100 × 100 × 400	7, 28	
Splitting tensile strength	Cylinder 150 × 300	7, 28	
Axial tensile strength	Prism 60 × 100 × 400	7, 28	
Modulus of elasticity	Cylinder 150 × 300	7, 28	

3. Experimental Results and Discussions

The results of slump and compressive strength tests are summarized in Table 5, where each value is an average result from three specimens for each GPC mix proportion, together with their coefficient of variation. Based on the experimental results, the effects of alkali-activator, water, and superplasticizer on the workability of one-part alkali-activated GPC paste, as well as on the compressive strength of the GPC, are discussed in detail below.

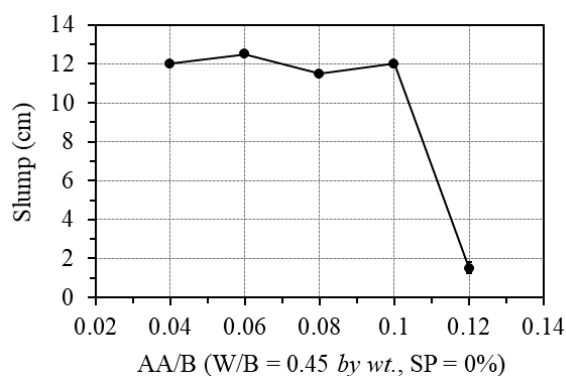
Table 5. Test results of mean slump and compressive strength of GPC.

Group	Specimens	Ratio				Slump (cm)	COV	3 Days		7 Days		28 Days	
		AA/B	W/B	H ₂ O/ Na ₂ O	SP (%)			f' _c (MPa)	COV	f' _c (MPa)	COV	f' _c (MPa)	COV
A	AA0.04-W0.45	0.04	0.45	27.90	0	12.0	4.4%	10.5	7.2%	19.3	3.6%	23.6	5.7%
	AA0.06-W0.45	0.06	0.45	19.90	0	12.5	6.9%	15.6	5.1%	23.7	2.6%	30.4	3.2%
	AA0.08-W0.45	0.08	0.45	17.44	0	11.5	3.8%	27.3	6.4%	33.6	3.9%	38.3	2.6%
	AA0.10-W0.45	0.10	0.45	12.60	0	12.0	5.0%	30.6	4.4%	40.2	4.4%	47.1	3.7%
	AA0.12-W0.45	0.12	0.45	10.80	0	1.5	6.7%			N/A			
B	AA0.08-W0.52	0.08	0.52	23.09	0	23.0	3.9%	21	4.7%	26.3	2.4%	30.9	4.4%
	AA0.08-W0.48	0.08	0.48	21.31	0	18.0	1.7%	25.4	6.6%	31.9	5.2%	36.2	4.8%
	AA0.08-W0.45	0.08	0.45	17.44	0	11.5	4.0%	27.3	3.1%	33.6	4.3%	38.3	1.8%
	AA0.08-W0.43	0.08	0.43	16.66	0	6.0	4.4%	33.6	3.9%	43.5	3.4%	49.7	3.1%
	AA0.08-W0.43-SP1.0	0.08	0.43	16.66	1.0	12.0	2.2%	33.9	3.9%	38.6	3.9%	45.1	5.7%
	AA0.08-W0.41-SP1.0	0.08	0.41	15.12	1.0	7.0	4.3%	35.6	1.3%	47.2	2.6%	52.6	2.7%
	AA0.08-W0.41-SP1.5	0.08	0.41	15.12	1.5	13.5	3.7%	34.9	4.2%	46.8	4.3%	51.7	3.0%
	AA0.08-W0.39-SP1.5	0.08	0.39	13.96	1.5	6.0	2.9%	36.9	4.0%	52.1	3.2%	56.3	3.1%
	AA0.08-W0.39-SP2.0	0.08	0.39	13.96	2.0	14.5	4.8%	36.7	5.7%	51.6	4.3%	55.7	2.8%
	AA0.08-W0.37-SP2.0	0.08	0.37	12.15	2.0	5.0	2.0%	38.7	3.9%	54.3	1.4%	59.2	1.5%
	AA0.08-W0.37-SP2.5	0.08	0.37	12.15	2.5	0.0	N/A			N/A			

COV: Coefficient of variation.

3.1. Effects of Alkali-Activator, Water, and Superplasticizer on Workability of One-Part Alkali-Activated GPC Paste

The effect of the one-part alkali-activator was examined by changing the AA/B ratio from 0.04 to 0.12, while the W/B was fixed at 0.45, and no superplasticizer was used. Figure 7 shows the effect of the one-part alkali-activator on the workability of GPC paste. As can be seen in this figure, when the percentage of the one-part alkali-activator was less than 10.0% of the binder weight, the workability of the GPC paste was unaffected. However, with the alkali-activator of 12.0% of the binder amount by weight (AA/B = 0.12), the workability of the mixture decreased very quickly, leading to the inability to cast specimens. The cause is that the polymerization reaction is exothermic; when the amount of activator is too large, it accelerates the evaporation time of water and immediately activates polymerization and calcium oxide reactions at the same time. These causes lead to the loss of GPC's workability, as also indicated in the previous works [26,27,40,41].

**Figure 7.** Effect of one-part alkali-activator on the workability.

The effect of water was examined by changing the W/B ratio from 0.43 to 0.52, while the AA/B was fixed at 0.08. Figure 8 shows the effect of the W/B ratio on the workability of GPC paste. As is seen from this figure, the W/B ratio by weight has a significant influence on the workability of GPC. For the ratio of fly ash to blast furnace slag of 1/3 in this study, the slump of GPC paste increased from 6 cm to 23 cm as the W/B ratio increased from 0.43 to 0.52. Moreover, the minimum W/B ratio should be at least 0.43 to ensure the workability and fabrication of samples when no superplasticizer is added.

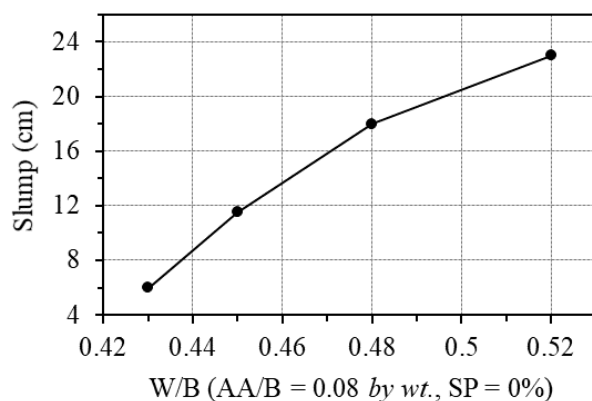


Figure 8. Effect of W/B ratio on the workability.

The effect of the superplasticizer was observed by changing the contents of this additive’s ratio from 0 to 2.5% of the total binder by weight (SP/B), while the AA/B was fixed at 0.08. Figure 9 shows the effect of the superplasticizer on the workability of GPC paste. It is seen that adding superplasticizers can greatly improve the workability of GPC. Indeed, for the mix proportion with a W/B ratio of 0.43, the slump of fresh GPC increased from 6 to 12 cm when the amount of superplasticizer was added to the mixture up to 1.0%. A similar trend was observed for the mix proportions with a W/B ratio of 0.41 and 0.39 when the added amount of superplasticizer increased from 1.0% to 1.5% and from 1.5% to 2.0%, respectively. The increase in slump with an increasing amount of superplasticizer could be due to the instability of the commercial superplasticizer in high basic media such as NaOH + Na₂SiO₃ [42]. In other words, according to Nematollahi and Sanjayan [30,42], the superplasticizer used in this study was chemically unstable in multi-compound activator (SiO₂/Na₂O = 2.1), and it experienced structural changes which resulted in the loss of their plasticizing characteristics. For the mix proportion with a W/B ratio of 0.37, due to the low amount of water, the superplasticizer just exhibited the effect on workability at a ratio of 2.0%. However, increasing the superplasticizer to 2.5% does not improve the workability. This value can be considered as the upper bound when using superplasticizer-based polyciliate for GPC.

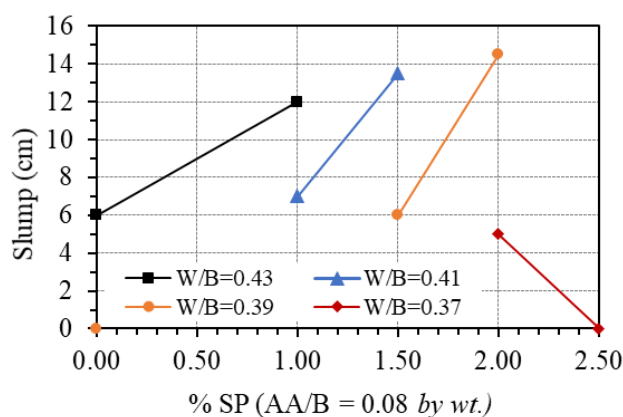


Figure 9. Effect of superplasticizer on the workability.

3.2. Effects of Alkali-Activator and Water on Compressive Strength of GPC

Figure 10 shows the effect of a one-part alkali-activator on the compressive strength of GPC at different days of age. As can be seen in this figure, the compressive strength increased with the increasing AA/B ratio. With the W/B ratio of 0.45, the compressive strength at 3 days increased by 48.6%, 75.0%, and 12.1% when the AA/B ratio changed from 0.04 to 0.06, 0.06 to 0.08, and 0.08 to 0.1, respectively. The corresponding increments of the

strength at 7 days were 22.8%, 41.8%, and 19.6%. However, the increments of compressive strength at 28 days of 28.8%, 25.8%, and 23.1% were quite similar when the AA/B ratio changed from 0.04 to 0.06, 0.06 to 0.08, and 0.08 to 0.1, respectively. These results indicate that the one-part alkali-activator has a significant effect on the compressive strength of GPC. The effect is relatively uniform for the strength at the age of 28 days but quite different for the strength at an early age, with the AA/B ratio from 0.04 to 0.1. The effect of the one-part alkali-activator on the compressive strength of GPC at 28 days was slightly decreased with the higher amount of the alkali-activator, whereas the amount of the alkali-activator corresponding to AA/B ratio from 0.06 to 0.08 exhibited the highest effect on the strength at 3 and 7 days. This can be explained as the pH level due to the amount of Na_2O in the alkali-activator in the range of 6% to 8% of total binder by weight is sufficient for the amount of Al_2O_3 and SiO_2 in fly ash and granulated blast furnace slag (FA/GBFS = 1:3) in this study. It is noted that using the activator up to 12% of the total binder amount by weight (AA/B = 0.12), specimens could not be cast due to the too-fast setting of GPC paste.

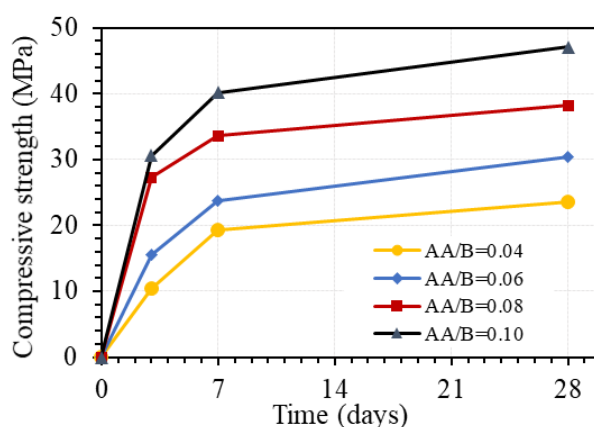


Figure 10. Effect of one-part alkali-activator on the compressive strength of GPC (W/B = 0.45 by weight, no superplasticizer).

The effect of water via the W/B ratio on the compressive strength of GPC at different days of age is displayed in Figure 11. This figure shows that the W/B ratio has a great effect on the compressive strength of GPC. For GPC with the AA/B ratio of 0.08 and without superplasticizer, the effect is quite similar for strength values at 3, 7, and 28 days but much different from various ranges of W/B ratio, as shown in Figure 11a. Indeed, the compressive strength at 3, 7, and 28 days decreased by an average of 9.4%, 11.4%, and 11.5% per 1% increase in the W/B ratio when the W/B ratio was between 0.43 and 0.45, respectively. However, the corresponding average reduction values of compressive strength per 1% increase in W/B ratio when W/B ratio between 0.45 and 0.48 was very low of 2.3%, 1.7%, and 1.8%, whereas higher values of 4.3%, 4.4%, and 3.7% were observed for mean reduction values of compressive strength at 3, 7, and 28 days per 1% increase in W/B ratio when W/B ratio between 0.48 and 0.52, respectively. Further, the compressive strength at 3, 7, and 28 days similarly decreased by 37.5%, 39.5%, and 37.8% when the W/B ratio increased from 0.43 to 0.52, respectively. This effect may be attributed to the following two causes. Firstly, reducing the amount of water leads to the reduction of excess water, which is one of the main causes of the formation of voids in GPC. Secondly, the $\text{H}_2\text{O}/\text{Na}_2\text{O}$ ratio decreases when the amount of water is reduced, leading to an increasing pH level. These phenomena lead to an increase in the compressive strength of GPC, which was also pointed out in the previous works [43–45].

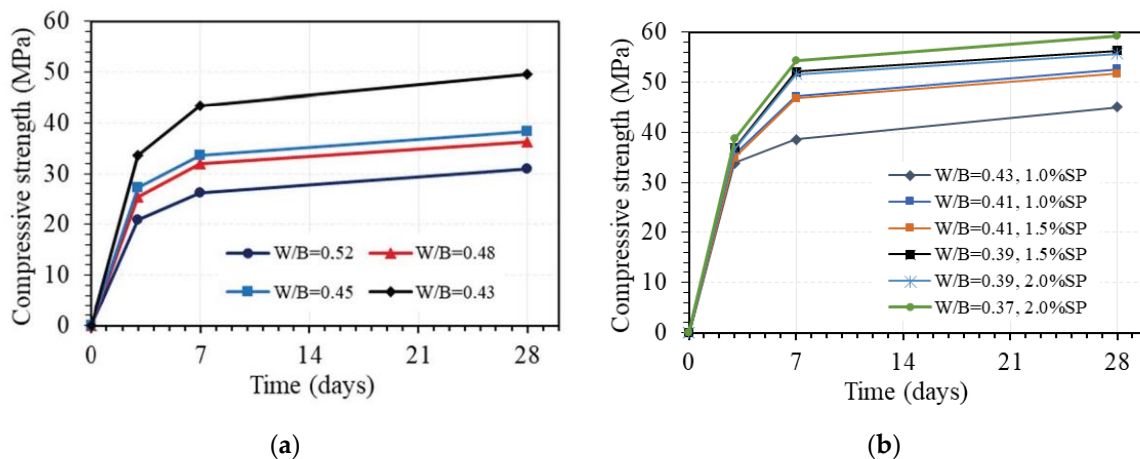


Figure 11. Effect of W/B ratio on compressive strength of GPC (AA/B = 0.08 by wt.): (a) without superplasticizer; (b) with superplasticizer.

When adding a superplasticizer to GPC, the effect of water via the W/B ratio on the compressive strength of GPC on different days is still great, as shown in Figure 11b. For instance, the compressive strength at 28 days of GPC with 1% superplasticizer decreased by 14.3% from 52.6 MPa to 45.1 MPa when the W/B ratio increased from 0.41 to 0.43. With 1.5% superplasticizer, the compressive strength at 28 days of GPC decreased by 8.2% from 56.3 MPa to 51.7 MPa when the W/B ratio increased from 0.39 to 0.41, while the strength at 28 days of GPC with 2% superplasticizer decreased by 5.9% from 59.2 MPa to 55.7 MPa when the W/B ratio increased from 0.37 to 0.39. From these results, a part of the influence of the superplasticizer on the compressive strength of GPC was also exhibited. With the same W/B ratio, adding a superplasticizer can enhance the workability but reduce the strength of GPC. For example, with a W/B ratio of 0.43, the compressive strength at 28 days of GPC decreased by 9.3% from 49.7 MPa to 45.1 MPa when adding 1% superplasticizer.

3.3. Compressive Strength Development under the Time of One-Part Alkali-Activated GPC in Comparison with OPC Concrete

The compressive strength development under the time of OPC concrete can be predicted using the equations given by two common codes, Eurocode2 [46] and ACI 209R [47], in which the compressive strength of OPC concrete at t days of age can be estimated from the compressive strength at 28 days.

Eurocode2 gives the equation for the development of compressive strength under the time of OPC concrete, as follows [46]:

$$f'_c(t) = \text{Exp} \left\{ s \left(1 - \left(\frac{28}{t} \right)^{1/2} \right) \right\} f'_c(28) \quad (4)$$

where $f'_c(t)$ and $f'_c(28)$ are the compressive strength at t and 28 days, respectively; s is a constant coefficient depending on the type of cement. For cement class N in OPC concrete, s is taken as 0.25.

In ACI 209R, the development of compressive strength development under the time for OPC concrete can be predicted using the following equation [47]:

$$f'_c(t) = \frac{t}{\alpha + \beta t} f'_c(28) \quad (5)$$

where α and β are coefficients, those depend on the cement type and curing condition, respectively. The constant α is set to 4 for cement type I while the constant β is taken as 0.85 for moist curing in this study.

For the purpose of comparison, the relationship between compressive strength at t days and 28 days of age is normalized to the strength value at 28 days. Figure 12 shows the development of normalized compressive strength under the time of GPC in the case of without superplasticizer (Figure 12a) and with added superplasticizer (Figure 12b), where the strength at 28 days of GPC is taken as 1.0. The corresponding curves drawn from prediction equations given by two common codes, Eurocode2 and ACI 209R, for OPC concrete are also plotted. As can be seen in Figure 12a, the development curves of compressive strength under the time of GPC using different W/B and no superplasticizer are almost identical, which proves that the compressive strength development of GPC follows a very stable trend, as well as the experimental results in this study, are highly reliable. However, at an early age, the compressive strength values of all specimens were slightly higher than the predicted values based on Eurocode2, while they were quite much higher than the ones obtained from ACI 209R for OPC concrete. It was reported in the previous work that the fly-ash-based geopolymer concrete with specific temperature and time-curing conditions achieves high early compressive strength due to the fast hydration reaction [40]. Moreover, the fast setting time and high early compressive strength of alkali-activated slag concrete due to the presence of high CaO content have also been shown in many other studies [43,48–50]. The obtained results in this work are consistent with the previous studies and could be used to investigate the creep and shrinkage properties of one-part alkali-activated GPC.

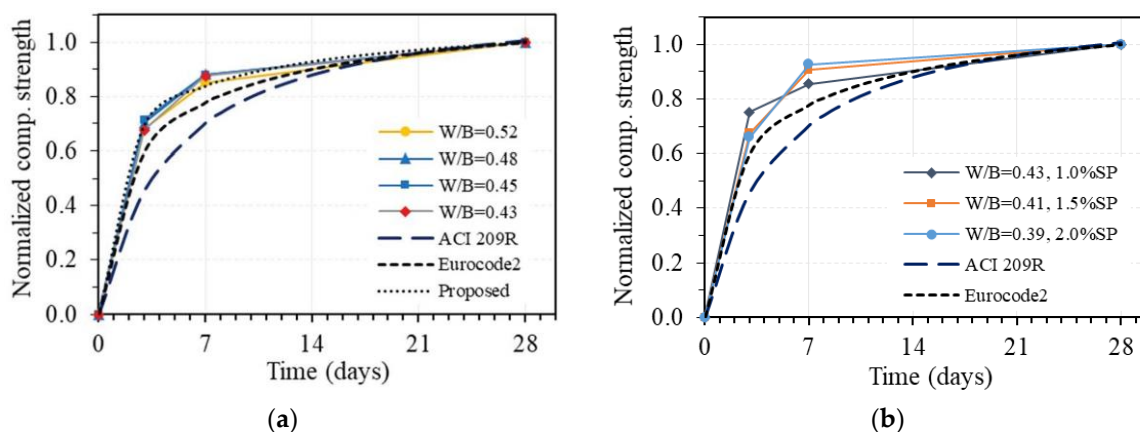


Figure 12. Compressive strength development under the time of one-part alkali-activated GPC in comparison with that of OPC concrete according to Eurocode 2 and ACI 209R: (a) without superplasticizer; (b) with superplasticizer.

Concerning the stable trend and high reliability of the obtained results, a prediction equation for compressive strength development of GPC without superplasticizer is proposed based on the original one from Eurocode2 [46], in which the constant s is taken as 0.175 instead of 0.25 for cement class N. The corresponding curve of the proposed equation is also plotted in Figure 12a, showing good agreement with the experimental results in this study. Adding an amount of superplasticizer to GPC leads to the change of development trend of compressive strength under the time of GPC, as shown in Figure 12b. This trend is different with various amounts of added superplasticizer to GPC; however, the compressive strengths at early ages of all specimens were always higher than the predicted values based on both Eurocode2 and ACI 209R codes. The obtained results indicate that superplasticizer has a significant effect on the development of compressive strength under the time of GPC, and another equation taking into account the effect of superplasticizer is required for predicting the compressive strength development of GPC, which may be conducted in future work.

3.4. Tensile Strengths, Modulus Elasticity, and Their Relations with Compressive Strength of One-Part Alkali-Activated GPC

After compressive strength tests had been carried out, three mix proportions, AA0.06-W0.45, AA0.08-W0.45, and AA0.10-W0.45, showed the compressive strength of about 30 MPa, 40 MPa, and 50 MPa were chosen to investigate the tensile strengths, modulus of elasticity as well as their relations with compressive strength of GPC. It should be noted that the three chosen mix proportions do not contain superplasticizers in order to be able to evaluate the relationship between the tensile strengths and modulus elasticity with compressive strength of pure one-part alkali-activated GPC. Figure 13 presents the results of the mean tensile strength of GPC from three specimens at 7 and 28 days with different testing types, including flexural, splitting, and axial tensile tests, which are also summarized in Table 6, together with their coefficient of variation.

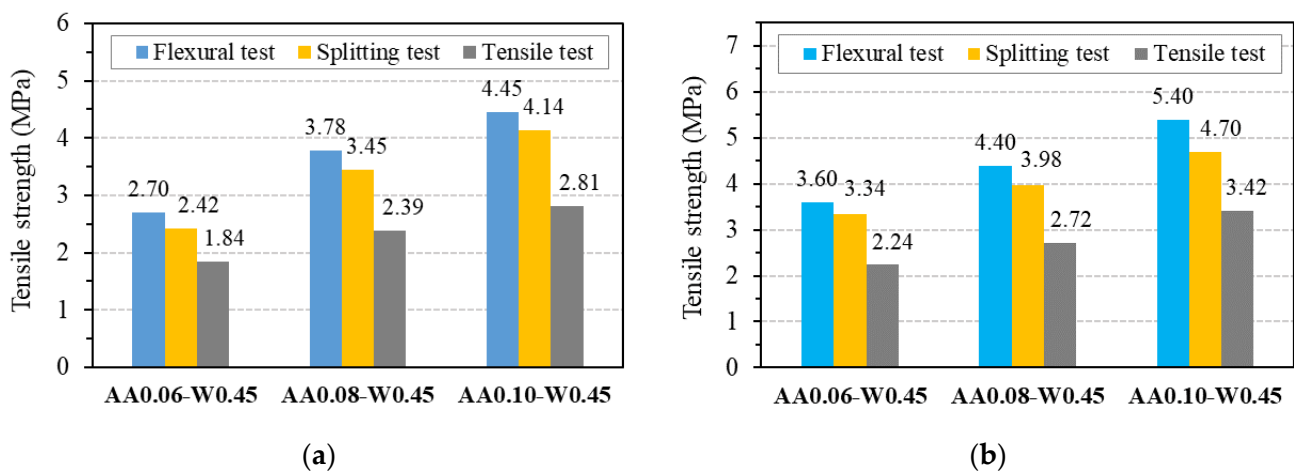


Figure 13. Tensile strength of GPC: (a) at 7 days; (b) at 28 days.

Table 6. Test results of mean tensile strength of GPC from different testing types.

Specimens	Testing Type	7 Days		28 Days	
		Value (MPa)	COV	Value (MPa)	COV
AA0.06-W0.45	Flexural test	2.70	3.7%	3.60	4.8%
	Splitting test	2.42	1.9%	3.34	3.2%
	Tensile test	1.84	9.5%	2.24	8.1%
AA0.08-W0.45	Flexural test	3.78	2.8%	4.40	2.3%
	Splitting test	3.45	1.5%	3.98	2.7%
	Tensile test	2.39	11.6%	2.72	3.5%
AA0.10-W0.45	Flexural test	4.45	3.0%	5.40	3.2%
	Splitting test	4.14	2.8%	4.70	2.8%
	Tensile test	2.81	3.4%	3.42	6.7%

COV: Coefficient of variation.

As can be seen from Figure 13, the splitting tensile strength is lower than flexural tensile strength and higher than the value obtained from the axial (direct) tensile test for all three mix proportions of GPC. This trend is similar to OPC concrete, as reported in common design codes such as ACI 318 [51] and Eurocode2 [46]. For the tensile strength at 7 days, the ratio between the values obtained from flexural tests and splitting tests was in the range from 1.07 to 1.12, whereas the ratio between the values obtained from direct tensile tests and splitting tests was in the range from 0.68 to 0.76. Similar ranges of from 1.08 to 1.15 and 0.67 to 0.73 were observed for flexural tensile strength/splitting tensile strength ratio and axial (direct) tensile strength/splitting tensile strength ratio at 28 days, respectively. These results indicate that the relationships between three types of tensile

strength of GPC are stable and reliable. These relationships will be explored through their relationship to the compressive strength of GPC, as detailed below.

According to ACI 318, the relationship between the splitting tensile strength (f_{ct}) and the compressive strength (f'_c) of concrete is expressed as [51]:

$$f_{ct} = 0.56\sqrt{f'_c} \text{ MPa} \quad (6)$$

The flexural tensile strength (f_r) and the compressive strength (f'_c) have the relationship as follows [51]:

$$f_r = 0.62\sqrt{f'_c} \text{ MPa} \quad (7)$$

According to Eurocode2, the relationship between the mean axial tensile strength (f_{ctm}) and the concrete cylinder compressive strength (f_{cm}) is provided as following relations [46]:

$$f_{ctm} = 0.3(f_{ck})^{2/3} \text{ MPa for } \leq C50/60 \quad (8)$$

$$f_{ck} = (f_{cm} - 8) \text{ MPa for } \leq C50/60 \quad (9)$$

where (f_{ck}) is the characteristic cylinder compressive strength of concrete.

Eurocode 2 also gives the association between the axial tensile strength (f_{ctm}) and the splitting tensile strength ($f_{ct,sp}$) as follows:

$$f_{ctm} = 0.9f_{ct,sp} \text{ MPa} \quad (10)$$

The association between mean flexural tensile strength ($f_{ctm,fl}$) and mean axial tensile strength is expressed as:

$$f_{ctm,fl} = \max \left[\left(1.6 - \frac{h}{1000} \right) f_{ctm}; f_{ctm} \right] \quad (11)$$

where h is the total member depth in mm.

The relationships between each type of tensile strength and compressive strength of concrete according to ACI 318 and Eurocode2 are drawn in Figure 14, together with the corresponding experimental results in this study for GPC.

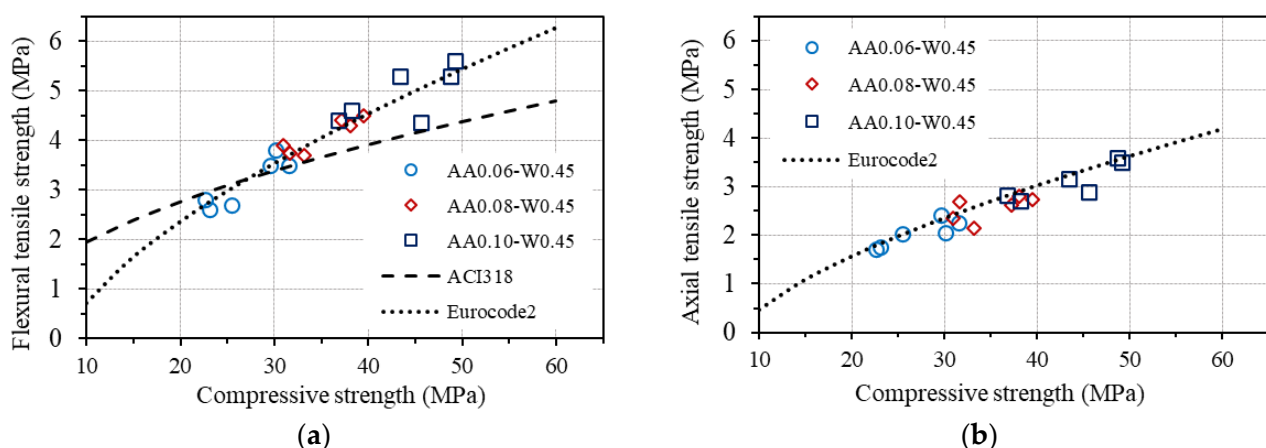


Figure 14. Cont.

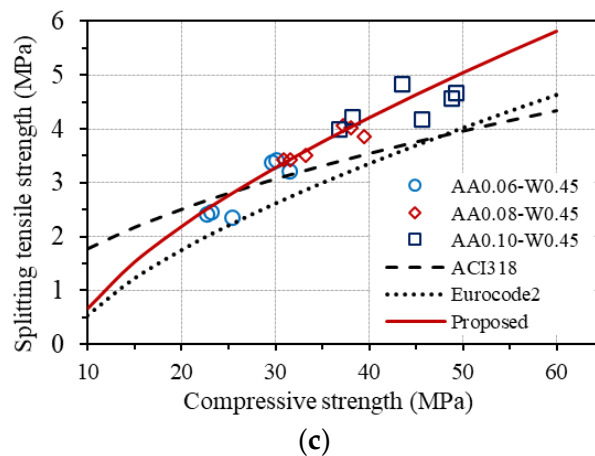


Figure 14. Relationship between tensile and compressive strengths: (a) flexural tensile strength; (b) Axial (direct) tensile strength; (c) splitting tensile strength.

As can be seen in Figure 14a, the measured flexural tensile strengths are quite different from the predictions by ACI 318 but agree well with that estimated by Eurocode2. A good agreement between the measured axial tensile strengths and the predicted values from compressive strength based on Eurocode2 is also observed, as shown in Figure 14b. These results confirm that the relationship between the flexural tensile strength and the compressive strength, as well as between the axial tensile strength and the compressive strength of concrete provided by Eurocode2, fits well with the investigated GPC in this study. However, a good agreement is not seen for the measured splitting tensile strength of GPC from both standards, as displayed in Figure 14c. Considering the conformity of the equations for estimating the flexural tensile strength and the axial tensile strength from the compressive strength of concrete provided by Eurocode2 to GPC, an equation for predicting splitting tensile strength from axial tensile strength of GPC is proposed, which is based on the original one in Eurocode2, as follows:

$$f_{ctm} = 0.72f_{ct,sp} \text{ MPa} \quad (12)$$

From the proposed equation, splitting tensile strength can be predicted from the compressive strength of GPC using the relationship between Equations (8) and (12), which is also plotted in Figure 14c, showing good agreement with the experimental results of splitting tensile strength of GPC.

Figure 15 presents the results of the mean elastic modulus of GPC from three specimens with three different mix proportions at 7 and 28 days, which are also summarized in Table 7, together with their coefficient of variation. As is seen from this figure, the elastic modulus at 7 days of age achieved about 85 to 88% of the values at 28 days of age, demonstrating the stable development of the modulus and the reliability of the experimental results. Based on that, the relationship between elastic modulus and compressive strength of GPC can be conducted.

Table 7. Test results of mean elastic modulus of GPC.

Specimens	7 Days		28 Days	
	<i>E</i> (GPa)	COV	<i>E</i> (GPa)	COV
AA0.06-W0.45	23.4	1.0%	27.6	0.5%
AA0.08-W0.45	28.1	0.7%	32.0	0.8%
AA0.10-W0.45	32.5	0.4%	37.2	1.4%

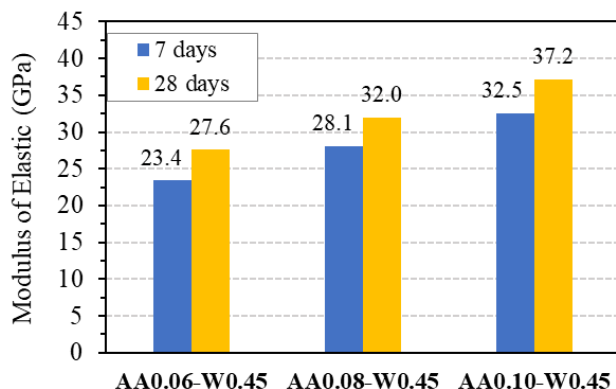


Figure 15. Elastic modulus of GPC.

The elastic modulus (E_c) can be estimated from the compressive strength (f'_c) of concrete according to ACI 318 as [51]:

$$E_c = 4700\sqrt{f'_c} \text{ MPa} \tag{13}$$

According to Eurocode2, the relationship between the elastic modulus (E_c) and the concrete cylinder compressive strength (f_{cm}) is given as [46]:

$$E_{cm} = 22 \left(\frac{f_{cm}}{10} \right)^{0.3} \text{ where } E_{cm} \text{ in GPA and } F_{cm} \text{ in MPA} \tag{14}$$

Figure 16 displays the curves drawn from the equations for estimating elastic modulus from the compressive strength of concrete provided by ACI 318 and Eurocode2, together with the measured elastic modulus of GPC. As seen, although the trend of the curve given by ACI 318 is relatively consistent with the experimental results of GPC, the prediction equations from both codes do not agree well with GPC. Based on that, a modification of the original equation from ACI 318 was made to fit the experimental results, as follows:

$$E_c = 5090\sqrt{f'_c} \text{ MPa} \tag{15}$$

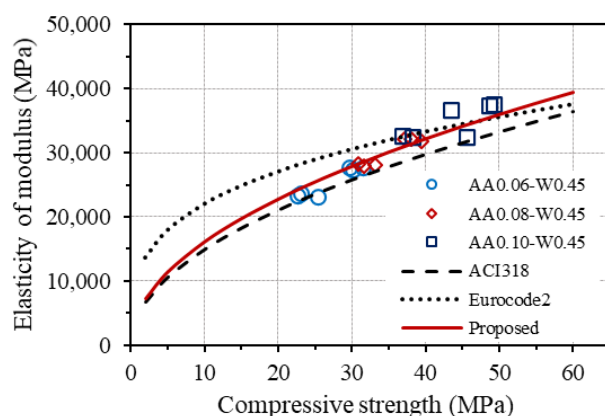


Figure 16. Relationship between elastic modulus and compressive strength.

The corresponding curve of the modified equation is also plotted in Figure 16, showing good agreement with the experimental results of the elastic modulus of GPC. However, it is worth noting that further investigation on both the elastic modulus and strengths of one-part alkali-activated GPC is necessary to suggest an appropriate equation between the splitting tensile strength as well as elastic modulus and compressive strength of GPC owing to the few samples and mixtures were conducted in this work.

4. Conclusions

This study presented an experimental investigation on the evaluation of the workability and mechanical properties of one-part alkali-activated GPC manufactured at room temperature. The obtained results support the following conclusions.

1. The amount of one-part alkali-activator less than 10.0% of the total binder amount by weight has no influence on the workability but has a strong effect on the compressive strength of GPC. The one-part alkali-activator should not exceed 12.0% of the total binder amount by weight ($AA/B = 0.12$) in order not to lose the workability of GPC. The effect of the one-part alkali-activator on the compressive strength of GPC at 28 days was slightly decreased with the higher amount of the alkali-activator, whereas the amount of the alkali-activator corresponding to AA/B ratio from 0.06 to 0.08 exhibited the highest effect on the strength at 3 and 7 days.
2. W/B ratio by weight has a significant influence on both the workability and compressive strength of GPC. The workability of GPC paste reduced as the W/B ratio increased. The compressive strength of GPC without superplasticizer decreased when the W/B ratio increased, and this effect of the W/B ratio was quite similar for compressive strength values at 3, 7, and 28 days but much different from different ranges of W/B ratio. The change of the W/B ratio from 0.43 to 0.45 has the greatest influence on compressive strength, and the minimum W/B ratio should be at least 0.43 to ensure workability and sample-making when no superplasticizer is added.
3. Adding superplasticizers can greatly improve the workability of GPC but reduce the strength of GPC. Increasing the superplasticizer up to 2.5% does not improve the workability, and this amount can be considered as the upper bound when using superplasticizer-based polyciliate for one-part alkali-activated GPC.
4. Compressive strengths at an early age of GPC are slightly higher than the predicted values based on Eurocode2, while they are quite much higher than the ones obtained from ACI 209R. The constant s that depends on the cement type should be taken as 0.175 for cement class N in the prediction equation for the compressive strength development under the time of one-part alkali-activated GPC according to the original equation for OPC concrete given by Eurocode2.
5. The relationship between flexural tensile strength and compressive strength, as well as between axial tensile strength and compressive strength provided by Eurocode2 for OPC concrete, fits well with one-part alkali-activated GPC, whereas the ratio between axial tensile strength and splitting tensile strength is found to be about 0.72 for GPC instead of 0.9 as given by Eurocode2 for OPC concrete.
6. The relationship between elastic modulus and compressive strength of one-part alkali-activated GPC is found to follow the trend given by ACI 318 for OPC concrete, but a higher coefficient of 5090 should be used instead of 4700 in order to accurately predict elastic modulus from compressive strength of GPC.

It is noted that the aforementioned are based on a very limited number of experiments. Further investigation on both the elastic modulus and strengths of one-part alkali-activated GPC is necessary.

Author Contributions: Conceptualization, T.-T.P.; methodology, T.-T.P. and N.-L.N.; software, T.-T.N. (Tuan-Trung Nguyen) and T.-T.N. (Trung-Tu Nguyen); validation, T.-T.P., N.-L.N., T.-T.N. (Tuan-Trung Nguyen), T.-T.N. (Trung-Tu Nguyen) and T.-H.P.; formal analysis, T.-T.P. and T.-H.P.; investigation, T.-T.N. (Tuan-Trung Nguyen) and T.-T.N. (Trung-Tu Nguyen); resources, T.-T.P. and N.-L.N.; data curation, T.-T.P. and T.-H.P.; writing—original draft preparation, T.-T.P. and T.-H.P.; writing—review and editing, T.-H.P.; visualization, N.-L.N.; supervision, T.-H.P.; project administration, T.-T.P.; funding acquisition, T.-T.P. All authors have read and agreed to the published version of the manuscript.

Funding: This research was funded by the Ministry of Education and Training of Vietnam, grant number B2022-XDA-10.

Data Availability Statement: The data presented in this study are available on request from the corresponding author.

Conflicts of Interest: The authors declare no conflict of interest.

References

1. McLellan, B.C.; Williams, R.P.; Lay, J.; van Riessen, A.; Corder, G.D. Costs and Carbon Emissions for Geopolymer Pastes in Comparison to Ordinary Portland Cement. *J. Clean. Prod.* **2011**, *19*, 1080–1090. [CrossRef]
2. Bernal, S.A.; Mejía de Gutiérrez, R.; Provis, J.L. Engineering and Durability Properties of Concretes Based on Alkali-Activated Granulated Blast Furnace Slag/Metakaolin Blends. *Constr. Build. Mater.* **2012**, *33*, 99–108. [CrossRef]
3. Glukhovskiy, V.D. Soil Silicates. *Gosstroyizdat Kiev*. **1959**, *154*. Available online: [https://scholar.google.com/scholar_lookup?title=Gruntosilikaty+\(Soil+Silicates\)&author=Glukhovskiy,+V.D.&publication_year=1959](https://scholar.google.com/scholar_lookup?title=Gruntosilikaty+(Soil+Silicates)&author=Glukhovskiy,+V.D.&publication_year=1959) (accessed on 15 July 2023).
4. Krivenko, P. Synthesis of Cementitious Materials of the Me₂O-MeO-Me₂O₃-SiO₂-H₂O System with Required Properties. 1986. Available online: https://scholar.google.com/scholar?cluster=2495372416308018022&hl=vi&as_sdt=2005&scioldt=0,5 (accessed on 15 July 2023).
5. Davidovits, J. Geopolymers: Inorganic Polymeric New Materials. *J. Therm. Anal. Calorim.* **1991**, *37*, 1633–1656. [CrossRef]
6. Komljenović, M.; Bašćarević, Z.; Bradić, V. Mechanical and Microstructural Properties of Alkali-Activated Fly Ash Geopolymers. *J. Hazard. Mater.* **2010**, *181*, 35–42. [CrossRef]
7. Kim, Y.Y.; Lee, B.-J.; Saraswathy, V.; Kwon, S.-J. Strength and Durability Performance of Alkali-Activated Rice Husk Ash Geopolymer Mortar. *Sci. World J.* **2014**, *2014*, 209584. [CrossRef] [PubMed]
8. Aiken, T.A.; Sha, W.; Kwasny, J.; Soutsos, M.N. Resistance of Geopolymer and Portland Cement Based Systems to Silage Effluent Attack. *Cem. Concr. Res.* **2017**, *92*, 56–65. [CrossRef]
9. Albitar, M.; Mohamed Ali, M.S.; Visintin, P.; Drechsler, M. Durability Evaluation of Geopolymer and Conventional Concretes. *Constr. Build. Mater.* **2017**, *136*, 374–385. [CrossRef]
10. Bakharev, T. Resistance of Geopolymer Materials to Acid Attack. *Cem. Concr. Res.* **2005**, *35*, 658–670. [CrossRef]
11. Sagoe-Crentsil, K.; Brown, T.; Taylor, A. Drying Shrinkage and Creep Performance of Geopolymer Concrete. *J. Sustain. Cem. Mater.* **2013**, *2*, 35–42. [CrossRef]
12. Kong, D.L.Y.; Sanjayan, J.G. Effect of Elevated Temperatures on Geopolymer Paste, Mortar and Concrete. *Cem. Concr. Res.* **2010**, *40*, 334–339. [CrossRef]
13. Sarker, P.K.; Kelly, S.; Yao, Z. Effect of Fire Exposure on Cracking, Spalling and Residual Strength of Fly Ash Geopolymer Concrete. *Mater. Des.* **2014**, *63*, 584–592. [CrossRef]
14. Almutairi, A.L.; Tayeh, B.A.; Adesina, A.; Isleem, H.F.; Zeyad, A.M. Potential Applications of Geopolymer Concrete in Construction: A Review. *Case Stud. Constr. Mater.* **2021**, *15*, e00733. [CrossRef]
15. Davidovits, J. Properties of Geopolymer Cements. In *Proceedings of the First International Conference on Alkaline Cements and Concretes, Scientific Research Institute on Binders and Materials*; Kiev State Technical University: Kiev, Ukraine, 1994; pp. 131–149. Available online: <http://www.geopolymer.org/wp-content/uploads/KIEV.pdf> (accessed on 15 July 2023).
16. Hajjaji, W.; Andrejkovičová, S.; Zanelli, C.; Alshaaer, M.; Dondi, M.; Labrincha, J.A.; Rocha, F. Composition and Technological Properties of Geopolymers Based on Metakaolin and Red Mud. *Mater. Des.* **2013**, *52*, 648–654. [CrossRef]
17. Rao, F.; Liu, Q. Geopolymerization and Its Potential Application in Mine Tailings Consolidation: A Review. *Miner. Process. Extr. Metall. Rev.* **2015**, *36*, 399–409. [CrossRef]
18. Yang, K.-H.; Song, J.-K.; Ashour, A.F.; Lee, E.-T. Properties of Cementless Mortars Activated by Sodium Silicate. *Constr. Build. Mater.* **2008**, *22*, 1981–1989. [CrossRef]
19. Nath, P.; Sarker, P.K. Effect of GGBFS on Setting, Workability and Early Strength Properties of Fly Ash Geopolymer Concrete Cured in Ambient Condition. *Constr. Build. Mater.* **2014**, *66*, 163–171. [CrossRef]
20. Hadi, M.N.S.; Farhan, N.A.; Sheikh, M.N. Design of Geopolymer Concrete with GGBFS at Ambient Curing Condition Using Taguchi Method. *Constr. Build. Mater.* **2017**, *140*, 424–431. [CrossRef]
21. Davidovits, P.J. 30 Years of Successes and Failures in Geopolymer Applications. Market Trends and Potential Breakthroughs. In *Proceedings of the Geopolymer 2002 Conference, Melbourne, Australia, 28–29 October 2002*; pp. 1–16.
22. Poloju, K.K.; Annadurai, S.; Manchiryal, R.K.; Goriparthi, M.R.; Baskar, P.; Prabakaran, M.; Kim, J. Analysis of Rheological Characteristic Studies of Fly-Ash-Based Geopolymer Concrete. *Buildings* **2023**, *13*, 811. [CrossRef]
23. Shen, Q.; Li, B.; He, W.; Meng, X.; Shen, Y. Associated Effects of Sodium Chloride and Dihydrate Gypsum on the Mechanical Performance and Hydration Properties of Slag-Based Geopolymer. *Buildings* **2023**, *13*, 1285. [CrossRef]
24. Malkawi, A.B. Effect of Aggregate on the Performance of Fly-Ash-Based Geopolymer Concrete. *Buildings* **2023**, *13*, 769. [CrossRef]
25. Matalkah, F.; Xu, L.; Wu, W.; Soroushian, P. Mechanochemical Synthesis of One-Part Alkali Aluminosilicate Hydraulic Cement. *Mater. Struct.* **2016**, *50*, 97. [CrossRef]
26. Hardjito, D.; Wallah, S.E.; Sumajouw, D.M.J.; Rangan, B. V Fly Ash-Based Geopolymer Concrete. *Aust. J. Struct. Eng.* **2005**, *6*, 77–86. [CrossRef]
27. Hardjito, D.; Rangan, B.V. Development and Properties of Low-Calcium Fly Ash-Based Geopolymer Concrete. *Res. Rep. GC* **2005**, *94*. Available online: <https://espace.curtin.edu.au/handle/20.500.11937/5594> (accessed on 15 July 2023).

28. Luukkonen, T.; Abdollahnejad, Z.; Yliniemi, J.; Kinnunen, P.; Illikainen, M. One-Part Alkali-Activated Materials: A Review. *Cem. Concr. Res.* **2018**, *103*, 21–34. [[CrossRef](#)]
29. Hajimohammadi, A.; van Deventer, J.S.J. Characterisation of One-Part Geopolymer Binders Made from Fly Ash. *Waste Biomass Valorization* **2017**, *8*, 225–233. [[CrossRef](#)]
30. Nematollahi, B.; Sanjayan, J. Effect of Superplasticizers on Workability of Fly Ash Based Geopolymer. In *InCIEC 2013: Proceedings of the International Civil and Infrastructure Engineering Conference 2013*; Hassan, R., Yusoff, M., Ismail, Z., Amin, N.M., Fadzil, M.A., Eds.; Springer: Singapore, 2014; pp. 713–719.
31. *EN 196-1*; Methods of Testing Cement-Part 1: Determination of Strength. TS En-CEN: Brussel, Belgium, 2016.
32. *ASTM C494/C494M*; Standard Specification for Chemical Admixtures for Concrete, Type D-Water-Reducing and Retarding Admixtures and Type G-Water-Reducing, High Range, and Retarding Admixtures. ASTM International: West Conshohocken, PA, USA, 2019.
33. Keke, S.; Xiaoqin, P.; Shuping, W.; Lu, Z. Design Method for the Mix Proportion of Geopolymer Concrete Based on the Paste Thickness of Coated Aggregate. *J. Clean. Prod.* **2019**, *232*, 508–517. [[CrossRef](#)]
34. *ASTM C29/C29M*; Standard Test Method for Bulk Density (“Unit Weight”) and Voids in Aggregate. ASTM International: West Conshohocken, PA, USA, 2017.
35. *ASTM C143-78*; Standard Test Method for Slump Of Portland Cement Concrete. ASTM International: West Conshohocken, PA, USA, 2017.
36. *ASTM C39*; Concrete Cylinder Compression Testing. ASTM International: West Conshohocken, PA, USA, 2021.
37. *ASTM C469/C469M-10*; Standard Test Method for Static Modulus of Elasticity and Poisson’s Ratio of Concrete in Compression. ASTM International: West Conshohocken, PA, USA, 2014.
38. *ASTM C78/C78M*; Standard Test Method for Flexural Strength of Concrete. ASTM International: West Conshohocken, PA, USA, 2018.
39. *ASTM C496/C496M-04*; Standard Test Method for Splitting Tensile Strength of Cylindrical Concrete Specimens. ASTM International: West Conshohocken, PA, USA, 2017.
40. Hardjito, D. Studies on Fly Ash-Based Geopolymer Concrete. Ph.D Thesis, Curtin University of Technology, Bentley, WA, Australia, 2005.
41. Nuruddin, M.F.; Demie, S.; Shafiq, N. Effect of Mix Composition on Workability and Compressive Strength of Self-Compacting Geopolymer Concrete. *Can. J. Civ. Eng.* **2011**, *38*, 1196–1203. [[CrossRef](#)]
42. Nematollahi, B.; Sanjayan, J. Effect of Different Superplasticizers and Activator Combinations on Workability and Strength of Fly Ash Based Geopolymer. *Mater. Des.* **2014**, *57*, 667–672. [[CrossRef](#)]
43. Lee, N.K.; Lee, H.K. Setting and Mechanical Properties of Alkali-Activated Fly Ash/Slag Concrete Manufactured at Room Temperature. *Constr. Build. Mater.* **2013**, *47*, 1201–1209. [[CrossRef](#)]
44. Criado, M.; Fernández-Jiménez, A.; de la Torre, A.G.; Aranda, M.A.G.; Palomo, A. An XRD Study of the Effect of the SiO₂/Na₂O Ratio on the Alkali Activation of Fly Ash. *Cem. Concr. Res.* **2007**, *37*, 671–679. [[CrossRef](#)]
45. Lloyd, R.R.; Provis, J.L.; van Deventer, J.S.J. Microscopy and Microanalysis of Inorganic Polymer Cements. 1: Remnant Fly Ash Particles. *J. Mater. Sci.* **2009**, *44*, 608–619. [[CrossRef](#)]
46. *EN 1992-1-1*; Eurocode 2 Design of Concrete Structures Part 1: General Rules and Rules for Buildings. British Standard Institution: London, UK, 2004.
47. *ACI 209R*; Prediction of Creep, Shrinkage, and Temperature Effects in Concrete Structures. In *ACI Manual of Concrete. Practice Part 1: Materials and General Properties of Concrete*. American Concrete Institute: Farmington Hills, MI, USA, 1992.
48. Collins, F.; Sanjayan, J.G. Early Age Strength and Workability of Slag Pastes Activated by NaOH and Na₂CO₃. *Cem. Concr. Res.* **1998**, *28*, 655–664. [[CrossRef](#)]
49. Collins, F.; Sanjayan, J.G. Early Age Strength and Workability of Slag Pastes Activated by Sodium Silicates. *Mag. Concr. Res.* **2001**, *53*, 321–326. [[CrossRef](#)]
50. Fernández-Jiménez, A.; Puertas, F. Setting of Alkali-Activated Slag Cement. Influence of Activator Nature. *Adv. Cem. Res.* **2001**, *13*, 115–121. [[CrossRef](#)]
51. *ACI CODE-318-19*; Building Code Requirements for Structural Concrete and Commentary. American Concrete Institute: Farmington Hills, MI, USA, 2019.

Disclaimer/Publisher’s Note: The statements, opinions and data contained in all publications are solely those of the individual author(s) and contributor(s) and not of MDPI and/or the editor(s). MDPI and/or the editor(s) disclaim responsibility for any injury to people or property resulting from any ideas, methods, instructions or products referred to in the content.